Jurnal Kejuruteraan 38(7) 2026: 3331-3338
https://doi.org/10.17576/jkukm-2026-38(7)-13

Comparative Analysis of Electron Acceleration Mechanisms During Magnetotail Reconnection

Nurumira Ashikin[a], Wai-Leong Teh[a*] & Mardina Abdullah[a,b]

[a]*Space Science Center, Institute of Climate Change*

[b]*Department of Electrical, Electronic and System Engineering, Faculty of Engineering and Built Environment,*

Universiti Kebangsaan Malaysia, Malaysia

[*]*Corresponding author: wteh@ukm.edu.my*

Received 19 February 2026, Received in revised form 24 May 2026
Accepted 24 June 2026, Available online 30 October 2026

ABSTRACT

Magnetic reconnection is a critical process in astrophysical environments responsible for converting magnetic energy into plasma kinetic energy, often manifested as particle acceleration. This study aims to determine the dominant mechanism responsible for electrons acceleration during magnetic reconnection by investigating the average properties of energetic electron acceleration in the magnetotail reconnection region, focusing on three key mechanisms: Fermi acceleration, Betatron acceleration, and acceleration by parallel electric field. Using Magnetospheric MultiScale (MMS) observations of seven magnetic reconnection events during 2015-2017 in the magnetotail, we evaluate and compare the reconnection rate, power density, and the electron acceleration rate associated with each mechanism. The analysis reveals that Betatron acceleration contributes most significantly, exhibiting higher average acceleration rates than the other two mechanisms while acceleration due to parallel electric fields contributes considerably less. Betatron acceleration has an average relative contribution of 76.6%, compared with 16.9% for the Fermi mechanism and 6.5% for the parallel electric field mechanism. Furthermore, reconnection events with enhanced particle acceleration rate generally coincide with enhanced power density, indicating that faster reconnection facilitates stronger and more efficient energy transfer to electrons. The event with high acceleration rates also coincide with relatively high reconnection rates (0.05 and 0.07). These results suggest that Betatron-type acceleration plays a dominant role in energetic electrons acceleration. The findings provide observational support for the mechanism responsible for electron acceleration and contribute to a better understanding of energy conversion and particle acceleration in collisionless plasmas.

Keywords: Magnetic reconnection; electron acceleration; acceleration rate; power density; reconnection rate

INTRODUCTION

Magnetic reconnection is a phenomenon that facilitates energy conversion, leading to the emission of heat and plasma acceleration by altering the topology of magnetic fields. Structures formed from this process such as flux ropes, which are a helical form of magnetic field, or magnetic islands, are effective in energizing particles. It has been recognized that electrons are primarily accelerated via three principal mechanisms: The Fermi process, the Betatron process and acceleration by parallel electric field. Previous studies have discussed about these electron acceleration mechanisms during magnetic reconnection either theoretically, through simulations or via in-situ observations (Eriksson et al. 2020; Ma et al. 2022; Sun et al. 2022). Acceleration by parallel electric fields occurs in the reconnection diffusion region, where electrons are directly accelerated by electric fields aligned with the magnetic field lines. The energetic electrons are primarily accelerated by the reconnection electric field in the vicinity of the X line and separatrices (Yu et al. 2024). Moving further away from the reconnection site, particles are proposed to undergo additional acceleration by the Fermi

or Betatron process. Fermi-type acceleration occurs when particles continuously gain energy by reflecting between curved magnetic fields, such as during circulation within magnetic islands or between converging flux ropes, leading to energy increases through head-on collisions with magnetic fluctuations. Betatron acceleration involves electrons gaining kinetic energy through fluctuations in magnetic field strength while conserving their magnetic moment as they spiral around the magnetic field lines. As the magnetic field lines contract or intensify, the decreasing gyroradius results in the perpendicular electrons acceleration, leading to an increase in kinetic energy (Dahlin et al. 2014; Sun et al. 2022).

While many studies focus on a single mechanism, there have been few reports of combined mechanisms acting together to accelerate electrons (Chien et al. 2023; Eriksson et al. 2020; Li et al. 2021; Ma et al. 2022; Zhong et al. 2020). Fu et al. (2013) reported that Betatron and Fermi acceleration are responsible for the electron energization in outflow jets during unsteady reconnection. Some studies have come to the conclusion that the particles within contracting magnetic islands or shrinking flux tube are accelerated via the Fermi mechanism, while local magnetic field compression at the dipolarization front results in Betatron acceleration, and parallel electric field are responsible for energy gain in reconnection exhaust and suprathermal electron in flux ropes (Ma et al. 2022). The energetic electrons in the reconnection diffusion region are first accelerated within the thin current sheet by parallel electric field and subsequently become trapped and further accelerated by Betatron and Fermi mechanisms in the secondary flux ropes. We assert that all three mechanisms contributed to electron acceleration; however, this paper focuses on identifying the dominant mechanism based on several parameters relevant to this study. We aim to address the unresolved question regarding the primary acceleration mechanism, as no consensus has yet been established on this topic and it remains an active area of research (Guo et al. 2020).

We examine three parameters: power density, acceleration rate and reconnection rate. Power density reflects the energy conversion between electromagnetic and kinetic forms during magnetic reconnection (Liu et al. 2025). The acceleration rate measures the energy gain of electrons in a specific volume due to acceleration mechanisms, indicating how rapidly particles acquire energy in the reconnection region (Jiang et al. 2021). The reconnection rate quantifies how rapidly magnetic flux breaks and reconnects. It is often normalized to a characteristic Alfvén speed and magnetic field and serves as an indicator for the efficiency of magnetic energy conversion. In summary, understanding the efficiency of magnetic reconnection requires knowledge of how fast reconnection occurs through the reconnection rate, the extent of energy conversion through power density estimation, and the mechanisms of particle acceleration through the acceleration rate. Although these parameters have been discussed previously, they are often addressed separately, limited to one or two acceleration mechanisms, or investigated primarily via simulations. In contrast, this study provides a comparative analysis of all three parameters using in-situ observations of multiple magnetotail reconnection events, with the aim of identifying the most efficient mechanism driving electron acceleration.

METHODOLOGY

We analyzed 7 magnetic reconnection events during 2015 to 2017 observed by Magnetospheric Multiscale, MMS. The satellite is a configuration of four spacecraft flying in tetrahedron configuration. We analyzed burst-mode plasma measurements obtained from several instruments onboard the MMS spacecraft. The magnetic field data were provided by the Fluxgate Magnetometer (Russell et al. 2016). Plasma moments and velocities were obtained from the Fast Plasma Investigation (Pollock et al. 2016). Electric field data measurements were collected using the Electric Double Probe (Ergun et al. 2016). All vector components presented in this paper are expressed in the geocentric solar ecliptic (GSE) coordinate system.

It is essential to define the three key parameters analyzed in this paper: power density, acceleration rate, and reconnection rate. Power density is calculated using the equation $E \cdot J$, which requires deriving the electric field, E, from Ohm's law, $v \times B$, while the current density, J, is determined using the curlometer technique. The curlometer method is a way to estimate current density by evaluating the gradient of the magnetic field from multispacecraft measurements, which is crucial for determining magnetic curvature in the calculation of acceleration rate as well. All four spacecrafts simultaneously measure the magnetic field, allowing the computation of 'curl B' from which the current density is derived as $J=\nabla \times B/\mu_o$ (Dunlop et al. 2021). Estimation depends on the size and shape of the spacecraft's tetrahedron, where it is better if the shape is equilateral and current density structure smaller than the tetrahedron cannot generally be resolved. It is believed to produce better results than single spacecraft data estimation. The quantity $E \cdot J$ then represents the energy dissipation per unit time and volume. Hamrin et al. (2015) demonstrated that this parameter can be used to identify potential magnetic reconnection region as a zone that corresponds to a load that manifests itself as power density.

EQUATIONS

The electron acceleration rates of the Betatron mechanism, first-order Fermi mechanism due to curvature drift, and parallel electric field, E|| are calculated using the following equations, respectively (Dahlin et al. 2014; Ma et al. 2020; Zhong et al. 2020). We note that the measured electric field data are used instead of estimation.

$$ar_{betatron} = Pe_{\perp} v_{E\times B} \cdot \frac{\nabla B}{B} + \frac{P_{e\perp}}{B}\frac{\partial B}{\partial t} \quad (1)$$

$$ar_{fermi} = \left(P_{e\parallel} + n_e m_e v_{\parallel}^2\right) v_{E\times B} \cdot (b \cdot \nabla b) \quad (2)$$

$$ar_{parE} = J_{e\parallel} E_{\parallel} + \frac{\beta_{\perp}}{2} J_{\parallel} E_{\parallel} \quad (3)$$

Equations (1) to (3) together constitute the change of electron energy over time or the total energy gain of electrons in a unit volume per unit time (Ma et al. 2022; Jiang et al. 2021). P_e represents the electron pressure and b is the unit vector along the magnetic field. n_e denotes the electron density while m_e is the mass of electron. The subscript ∥ and ⊥ indicates the direction parallel and perpendicular to the background magnetic field, respectively. $\beta_{\perp}$ is defines as the ratio of the perpendicular electron pressure to the magnetic pressure, $\beta_{\perp} = \frac{P_{e\perp}}{B^2/2\mu_0}$.

The magnetic reconnection rate, $R=E_y\sqrt{\mu_0 mn}/B_{lobe}^2$ gives direct information about how fast the process goes and also how much magnetic flux is reconnected in time. This allows one to calculate how much magnetic energy is released in a given time (Hesse & Cassak 2020). The dominant acceleration mechanism is distinguished by analysing the average value of the power density, reconnection rate and the energy gain or acceleration rate for each event.

RESULTS AND DISCUSSION

We will first examine one of the events with the purpose of illustrating the variations of field data involving the related parameters during magnetic reconnection. Figure 1 shows the overview of an event observed by MMS on 18 July 2017 at 014130 UT – 014150 UT. From the top to the bottom panels, Figure 1 shows, (a)-(d) the magnitude and the x,y,z component of the magnetic field, while (e)-(g) are the x,y,z component of the ion velocity over the four spacecraft, respectively. Figure 2 shows the details of the plasma moment, where (a)-(c) are the x,y,z-component of electron velocity, (d)-(f) x,y,z direction of electric field and (g) is the plasma density. The color codes for each spacecraft are C1: black, C2: red, C3: green and C4: blue.

All of the spacecraft were in the northern hemisphere of the magnetotail (Bx>0). Based on the characteristics reversal value of z-axis magnetic field, B_z on Figure 1(d), the spacecraft passed through a reconnection x-line or a plasmoid. This is supported by the increase of magnetic field strength around 014140 UT when B_z changed bipolarly. The structure move earthward as the correlated reversal value of B_z and v_x in Figure 1(e) changes from negative to positive, with peak velocity of 600km/s while electron velocity reached 5000 km/s in Figure 2(a). Figure 2(g) shows that the plasma density increase within the plasmoid in accordance to the movement of the particles.

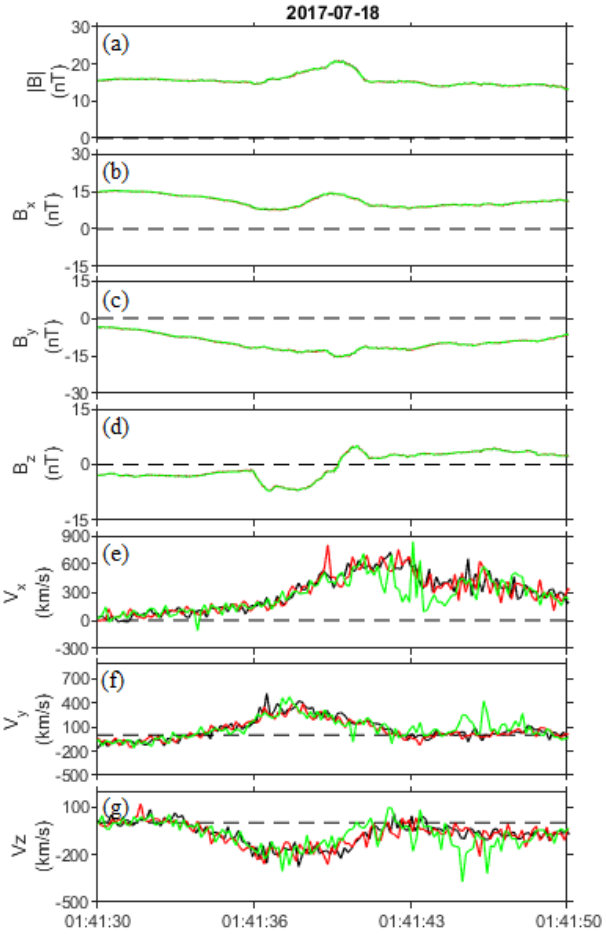


FIGURE 1. Overview of the magnetic reconnection event on 18 July 2017 around 014130-014150 UT. (a) magnitude of magnetic field, (b)-(d) x,y,z-component of magnetic field. (e)-(g) x,y,z-component of ion velocity.

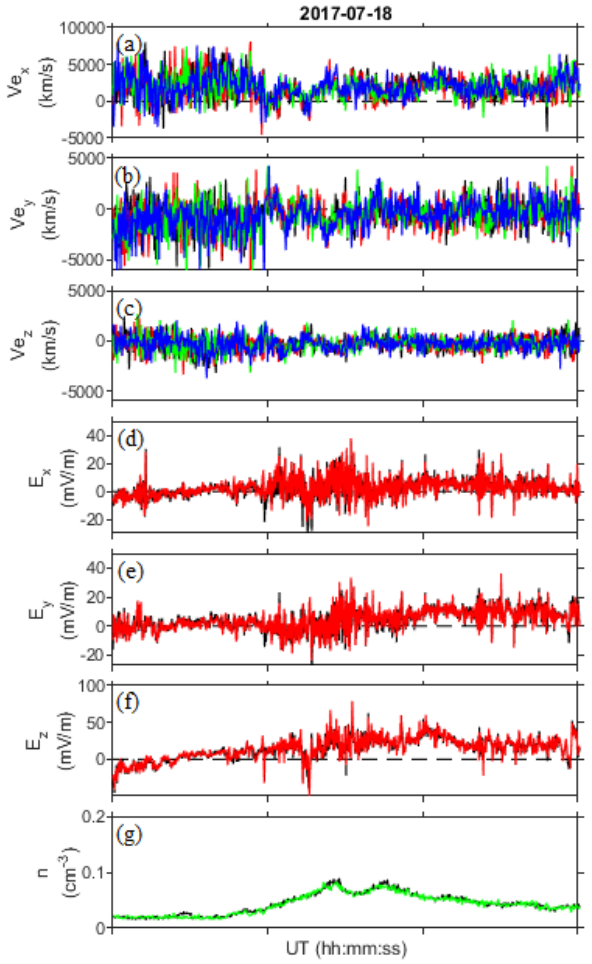


FIGURE 2. Observations of the (a)-(c) x,y,z-component of electron velocity, (d)-(f) x,y,z-component of electric field and (g) plasma density at the same date and time interval.

Figure 3 shows the (a) parallel pressure, (b) perpendicular pressure, (c) current density, (d) power density, and acceleration rate by (e) Betatron mechanism, (f) Fermi mechanism and (g) parallel electric field, respectively. There is an increase of parallel and perpendicular pressure which corresponds to the enhancement of acceleration rate by Fermi-type and Betatron mechanisms, respectively. The power density in panel 3(d) fluctuates between positive and negative values throughout the interval. Positive values correspond to periods of net energy transfer from the magnetic field to the plasma, indicating plasma energization, whereas negative values represent intervals of energy transfer from the plasma back to the field. On average, the power density remains positive, suggesting that the plasma gains energy overall.

In Figure 3(e), Betatron acceleration peaked around 014140 UT in the middle of plasmoid coinciding with the increased observed magnetic field strength and pressure within the plasmoid (see Figure 1(a) and 1(b)), while Fermi acceleration in Figure 3(f) increased after 014140 UT following the onset of reconnection and continuing until the end of x-line interval. Figure 3(e) and 3(f) shows that electrons were mainly accelerated by both Betatron and Fermi-type mechanisms. The contribution of the parallel electric field to electron acceleration in Figure 3(g) was found to be negligible, as its magnitude was too small. This is supported by Zhong et al. (2020), who reported that Betatron acceleration is more effective in energizing electrons to higher energies within these structures based on the comparisons of acceleration rates during the minutes preceding and following the observed interval due to the presence of flux ropes.

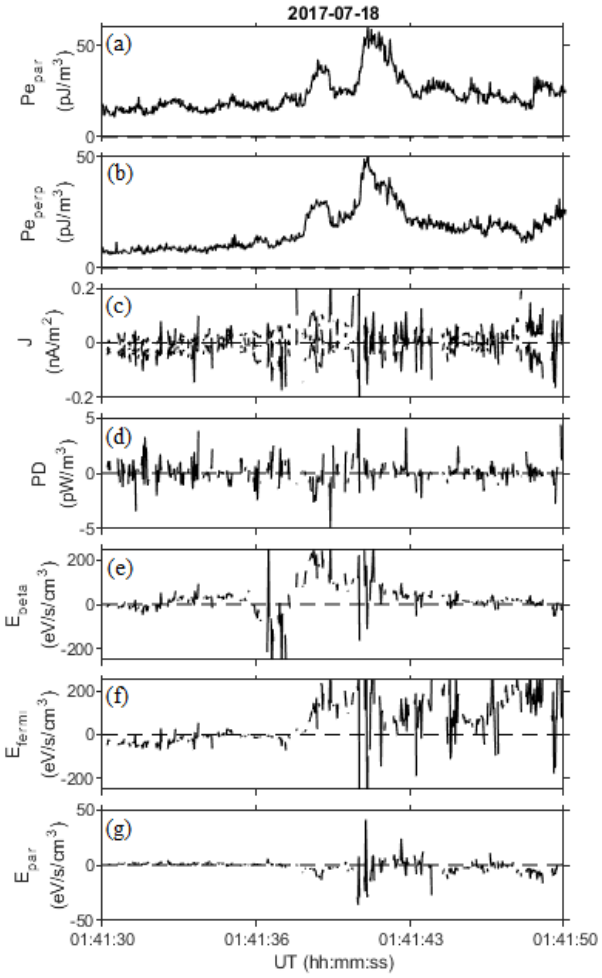


FIGURE 3. Measurements of the (a) parallel pressure, (b) perpendicular pressure, (c) current density, (d) power density, and acceleration rate by (e) Betatron (f) fermi mechanism and (g) parallel electric field at the same date and time interval.

In exploring the electron acceleration mechanisms, we calculated the average values of reconnection rate, power density and the acceleration rate for every event and

the results were recorded in Table 1. The term 'average' here denotes the mean of the measured values of respective parameters over the analysis interval for each event. The analysis of these magnetic reconnection events reveals that events with higher reconnection rates tend to correspond to higher acceleration rates. In contrast, events with lower reconnection rates exhibit lower power densities and acceleration rates. This suggests that stronger reconnection activity corresponds to more efficient energy transfer to plasma particles and that the acceleration processes occur more efficiently under fast reconnection conditions, where magnetic energy is rapidly converted into particle kinetic energy (Nakamura et al. 2018). The presence of one or two events with higher acceleration rates for Betatron and Fermi mechanisms reflects irregular and intense bursts of particle acceleration. The Betatron and Fermi acceleration mechanisms exhibit alternating periods of acceleration and deceleration. These bursts indicate that while Betatron and Fermi typically operate at fast rates, they are capable of driving much more rapid electron acceleration under certain conditions, such as strong energy dissipation and magnetic field compression around flux ropes and X-lines (Sun et al. 2022).

Negative acceleration rates observed in reconnection events listed in Table 1 can be attributed to several physical processes related to the dynamics of flux ropes and the structure of the reconnection region. One contributing factor is the role of the pressure tensor which enables energy transfer to the electromagnetic field, particularly during interactions with electric fields induced by decreasing magnetic field (Xiong et al., 2022). This can be observed in Figure 3(e), where the acceleration rate increased as the pressure increased in Figure 3(a)-(b) around 014138 UT and decreased as the pressure declined after 014143 UT. Furthermore, the spatial variation of acceleration efficiency within a flux rope can lead to localized deceleration. In Figure 3(f), where the acceleration rate was negative from 014130 UT until 014137 UT and became positive afterwards, suggesting the electrons were initially decelerated before subsequently undergoing acceleration. This is supported by previous studies showing that Fermi acceleration may become negative at the leading edge of a flux rope and positive at the trailing edge indicating a dynamic energy exchange process (Zhong et al. 2022). Additional causes to negative acceleration includes compressibility effects, where plasma heating occurs through compression, and current-energy balance mechanisms in the diffusion region, both of which can reduce the net energy gain of electrons (Liu et al., 2024).

TABLE 1. Summary of the average reconnection rate, power density and acceleration rate for Betatron, Fermi mechanism and acceleration by parallel electric field for seven reconnection events

Date and Time (UT)	Reconnection Rate	Average Power Density (pW/m^3)	Average Acceleration Rate ($eV/s/cm^3$)		
			Betatron Mechanism	Fermi Mechanism	Parallel Electric field
18/7/2017 0140-0142	0.0290	12.5776	-125.2313	8.6857	0.7743
5/10/2015 1145-1148	0.0712	74.1574	189.9685	-78.854	8.270
11/7/2017 2233-2235	0.0292	-0.9353	-33.8662	-38.2866	-57.4704
10/8/2017 1218-1220	0.0238	-5.8867	-184.0235	2.734	1.695
22/10/2016 1258-1300	0.0341	-216.4020	57.8191	20.8938	2.4208
26/7/2017 0710-0750	0.0503	-56.5719	373.8088	74.006	-14.9115
17/6/2017 2023-2025	0.0214	-0.8630	-48.2590	0.123	-0.184

Many studies have proposed Fermi acceleration, Betatron acceleration and parallel electric field as acceleration mechanism based on kinetic simulation and observational data (Wang et al., 2017; Zhou et al., 2018; Zhong et al. 2020). Previous studies have also shown that different mechanisms are active in different regions and can energize electrons during magnetic reconnection (Zhou et al. 2019; Eriksson et al. 2020; Norgren et al. 2020). Wu et al. (2015) proposed that electrons are initially accelerated at the x-line by parallel electric field into the reconnection exhaust, followed by further energization in the pileup region in the immediate downstream region and subsequently within the outflow region by Fermi or Betatron mechanism. The results in Table 1 shows that high power density tends to correspond to enhanced Betatron-type acceleration rate, indicating stronger energy gain through the Betatron mechanism, which is proportional to particle energy. This suggests that the Betatron mechanism is more effective in facilitating energy conversion and particle energization during reconnection. In contrast, negative power density values are generally associated with low acceleration rate driven by parallel electric field. This suggests that, rather than contributing significantly to particle energization, the energy transfer

may instead be directed back to the electromagnetic field or may contribute to particle deceleration, thereby limiting the generation of high-energy electron populations (Chien et al. 2023; Eriksson et al. 2020).

In the context of magnetic reconnection, Fermi and Betatron acceleration are considered the dominant acceleration mechanisms, while the parallel electric field primarily contribute to particle heating (Oka et al. 2023). Hence, calculating only the average of the parameters may fully capture temporally sensitive changes in magnetic field strength, which affect energy variation and event-to-event variability. Moreover, the average contribution should be interpreted as an overall trend rather than a universal characteristic of all reconnection events. Nevertheless, based on the obtained results, we conclude that Betatron is the primary mechanism responsible for electron acceleration during the analyzed magnetic reconnection events. This conclusion is further supported by standard statistical analysis of the acceleration rate for each mechanisms, as presented in Table 2 below. We note that the average reported in Table 2 represents the mean calculated over the seven MMS reconnection events.

TABLE 2. Summary of the statistical analysis for acceleration rate of Fermi, Betatron and by parallel electric field

Statistics	Description	Formula	Betatron	Fermi	Parallel Electric field
Mean	Average values for acceleration rate	$\Sigma xi / n$	31.4	-1.5	-8.5
Standard deviation	Measures how spread out the data is from the mean	$\sqrt{[\Sigma(xi-\bar{x})^2/n]}$	180.7	50.2	22.7
Min	Minimum values	min(x)	-184.0	-78.9	-57.5
Max	Maximum values	max(x)	373.8	74.0	8.3
Average relative contribution percentage based on acceleration rate	Shows what fraction of the total acceleration (in absolute terms) comes from each mechanism	$\Sigma(\|xi\|/\Sigma\|x\|)/n$	76.6%	16.9%	6.5%

The average relative contribution percentage were calculated by dividing the average accelerate rate for each mechanism by the sum of the absolute value for all mechanisms for each event. For example, on 18 July 2017, the Betatron relative contribution percentage was calculated as |-125.2313|/(|-125.2313| + |8.6857| + |0.7743|) x 100% = 93.0%. The values obtained for all events were then averaged to produce the data presented in Table 2. Since some mechanisms exhibit negative values, absolute values were used to account for the magnitude of the contribution regardless of direction. The Betatron mechanism exhibits the strongest overall contribution, with a mean acceleration rate of 31.4 eV/s/cm^3. The dominance of Betatron mechanism indicates that magnetic field compression plays a primary role in electron energization within the analyzed reconnection intervals. The relatively large standard deviation implies substantial variability among events, further suggesting that magnetic pile-up and dipolarization fronts may significantly enhance perpendicular electron energization.

The present results have important implications for understanding energy conversion during collisionless magnetic reconnection. By demonstrating the relative contribution of acceleration mechanisms in the analyzed magnetotail events, this study provides observational constraints for future theoretical and numerical models of electron energization.

CONCLUSION

In summary, we studied the average properties of energetic electrons associated with three acceleration mechanisms: Fermi acceleration, Betatron acceleration and acceleration by parallel electric field in the magnetotail reconnection region. We examined three main parameters related to these acceleration mechanisms: reconnection rate, power density and acceleration rate. The results presented in this study provide new insights into electron acceleration mechanisms, particularly in identifying which of the three acceleration mechanisms is the dominant driver of accelerating particle during magnetic reconnection. Understanding these electron acceleration mechanisms is important for advancing our knowledge of energy transfer and plasma dynamics. We analyzed seven MMS reconnection events observed between 2015 to 2017 in magnetotail region. Our results indicate that the Betatron mechanism plays the dominant role in electron acceleration during magnetic reconnection as it exhibited higher acceleration rate

compared to other mechanisms. Furthermore, the particle acceleration rate increases with power density, suggesting that greater available energy enhances energy transfer to charged particles. Thus, faster reconnection processes facilitate stronger and more efficient particle acceleration within the plasma environment. These findings may help improve and strengthen the current understanding of this unresolved problem. For future work, the analysis could be extended to include power-law spectra and pitch-angle anisotropy as the present study did not consider particle heating or turbulence effects.

ACKNOWLEDGEMENT

This work was sponsored by a grant from Universiti Kebangsaan Malaysia (GP-K020730). Some part of the calculations was made possible with the help from irfu-matlab. We also thank NASA for the readily available MMS data.

DECLARATION OF COMPETING INTEREST

None.

REFERENCES

Chien, A., Gao, L., Zhang, S., Ji, H., Blackman, E.G., Daughton, W., Stanier, A., Le, A., Guo, F., Follett, R., Chen, H., Fiksel, G., Bleotu, G., Cauble, R.C., Chen, S.N., Fazzini, A., Flippo, K., French, O., Froula, D.H., Fuchs, J., Fujioka, S., Hill, K., Klein, S., Kuranz, C., Nilson, P., Rasmus, A. & Takizawa, R. 2023. Non-thermal electron acceleration from magnetically driven reconnection in a laboratory plasma. *Nature Physics* 19(2): 254–262. https://doi.org/10.1038/s41567-022-01839-x

Dahlin, J.T., Drake, J.F. & Swisdak, M. 2014. The mechanisms of electron heating and acceleration during magnetic reconnection. *Physics of Plasmas* 21(9): 092304. https://doi.org/10.1063/1.4894484

Dunlop, M.W., Dong, X.-C., Wang, T.-Y., Eastwood, J.P., Robert, P., Haaland, S., Yang, Y.-Y., Escoubet, P., Rong, Z.-J., Shen, C., Fu, H.-S. & De Keyser, J. 2021. Curlometer technique and applications. *Journal of Geophysical Research: Space Physics* 126(11): e2021JA029538. https://doi.org/10.1029/2021JA029538

Ergun, R.E., Tucker, S., Westfall, J., Goodrich, K.A., Malaspina, D.M., Summers, D., Wallace, J., Karlsson, M., Mack, J. & Brennan, N. 2016. The axial double probe and fields signal processing for the MMS mission. *Space Science Reviews* 199: 167–188. https://doi.org/10.1007/s11214-014-0115-x

Eriksson, E., Vaivads, A., Alm, L., Graham, D.B., Khotyaintsev, Y.V. & André, M. 2020. Electron acceleration in a magnetotail reconnection outflow region using Magnetospheric Multiscale data. *Geophysical Research Letters* 47(1):e2019GL085080. https://doi.org/10.1029/2019GL085080

Fu, H.S., Khotyaintsev, Y.V., Vaivads, A., Retinò, A. & André, M. 2013. Energetic electron acceleration by unsteady magnetic reconnection. *Nature Physics* 9(7): 426–430. https://doi.org/10.1038/nphys2664

Guo, F., Liu, Y.-H., Li, X., Li, H., Daughton, W. & Kilian, P. 2020. Recent progress on particle acceleration and reconnection physics during magnetic reconnection in the magnetically-dominated relativistic regime. *Physics of Plasmas* 27(8): 080501. https://doi.org/10.1063/5.0012094

Jiang, K., Huang, S.Y., Yuan, Z.G., Deng, X.H., Wei, Y.Y., Xiong, Q.Y., Xu, S.B., Zhang, J., Zhang, Z.H., Lin, R.T. & Yu, L. 2021. Statistical properties of current, energy conversion, and electron acceleration in flux ropes in the terrestrial magnetotail. *Geophysical Research Letters* 48(11): e2021GL093458. https://doi.org/10.1029/2021GL093458

Li, X., Guo, F. & Liu, Y.-H. 2021. The acceleration of charged particles and formation of power-law energy spectra in nonrelativistic magnetic reconnection. *Physics of Plasmas* 28(5): 052905. https://doi.org/10.1063/5.0047644

Liu, Y.-H., Hesse, M., Genestreti, K., Nakamura, R., Burch, J.L., Cassak, P.A., Bessho, N., Eastwood, J.P., Phan, T. & Swisdak, M. 2025. Ohm's law, the reconnection rate, and energy conversion in collisionless magnetic reconnection. *Space Science Reviews* 221(1): 16. https://doi.org/10.1007/s11214-025-01142-0

Ma, W., Zhou, M., Zhong, Z. & Deng, X. 2022. Contrasting the mechanisms of reconnection-driven electron acceleration with in situ observations from MMS in the terrestrial magnetotail. *The Astrophysical Journal* 931(2): 135. https://doi.org/10.3847/1538-4357/ac6be6

Oka, M., Birn, J., Egedal, J., Guo, F., Ergun, R.E., Turner, D.L., Khotyaintsev, Y., Hwang, K.-J., Cohen, I.J. & Drake, J.F. 2023. Particle acceleration by magnetic reconnection in geospace. *Space Science Reviews* 219(8): 75. https://doi.org/10.1007/s11214-023-01011-8

Pollock, C., Moore, T., Jacques, A., Burch, J., Gliese, U., Saito, Y., Omoto, T., Avanov, L., Barrie, A. & Coffey, V. 2016. Fast plasma investigation for Magnetospheric Multiscale. *Space Science Reviews* 199: 331–406. https://doi.org/10.1007/s11214-016-0245-4

Russell, C.T., Anderson, B.J., Baumjohann, W., Bromund, K.R., Dearborn, D., Fischer, D., Le, G., Leinweber, H.K., Leneman, D. & Magnes, W. 2016. The Magnetospheric Multiscale magnetometers. *Space Science Reviews* 199: 189–256. https://doi.org/10.1007/s11214-014-0057-3

Sun, W., Turner, D.L., Zhang, Q., Wang, S., Egedal, J., Leonard, T., Slavin, J.A., Hu, Q., Cohen, I.J., Genestreti, K., Poh, G., Gershman, D.J., Smith, A., Le, G., Nakamura, R., Giles, B.L., Ergun, R.E. & Burch, J.L. 2022. Properties and acceleration mechanisms of electrons up to 200 keV associated with a flux rope pair and reconnection X-lines around it in Earth's plasma sheet. *Journal of Geophysical Research: Space Physics* 127(12): e2022JA030721. https://doi.org/10.1029/2022JA030721

Yu, X., Lu, Q., Wang, R., Zhang, X. & Zhu, C. 2024. Observation of energetic electron near the electron diffusion region of magnetic reconnection. *Journal of Geophysical Research: Space Physics* 129(5): e2024JA032419. https://doi.org/10.1029/2024JA032419

Zhong, Z.H., Zhou, M., Tang, R.X., Deng, X.H., Turner, D.L., Cohen, I.J., Pang, Y., Man, H.Y., Russell, C.T., Giles, B.L., Paterson, W.R., Khotyaintsev, Y. & Burch, J.L. 2020. Direct evidence for electron acceleration within ion-scale flux rope. *Geophysical Research Letters* 47(1): e2019GL085141. https://doi.org/10.1029/2019GL085141